Effect of threading dislocations on carrier mobility in AlGaN/GaN quantum wells

2008 J. Phys.: Condens. Matter 20 325210

(http://iopscience.iop.org/0953-8984/20/32/325210)

IOP Publishing Journal of Physics: Condensed Matter

J. Phys.: Condens. Matter **20** (2008) 325210 (9pp) doi:10.1088/0953-8984/20/32/325210

Effect of threading dislocations on carrier mobility in AlGaN/GaN quantum wells

F Carosella[1] **and J-L Farvacque**

Laboratoire de Structure et Propriétés de l'Etat Solide (CNRS UMR 8008),
Université des Sciences et Technologies de Lille, 59655 Villeneuve d'Ascq Cedex, France

E-mail: francesca.carosella@u-psud.fr

Received 28 February 2008, in final form 17 June 2008
Published 9 July 2008
Online at stacks.iop.org/JPhysCM/20/325210

Abstract

The various scattering mechanisms induced by dislocations have been reviewed and adapted to the case of threading dislocations in AlGaN/GaN quantum wells. These scattering mechanisms can be classified into two categories, the first one issuing straightforwardly from the dislocation strain field, the other one being due to the Coulomb potential created by electrons trapped on the energy states that dislocations may create in the GaN band gap. For the first category of mechanisms (strain field effects), we indicate that edge dislocations can only be connected with the so-called deformation potential, the piezoelectric coupling being ruled out because of the particular geometry of the threading dislocation strain fields. We show that the dislocation deformation potential can only be responsible for a very weak, even negligible, effect on the carrier mobility. Then, after a survey of the various results found in the literature concerning the possible existence of dislocation energy states we conclude that dislocations are responsible for the existence of shallow acceptor states below the conduction band and propose a model for describing the potential associated with such states when filled by electrons. More particularly, we show that the linear dislocation charge density resulting from the trapped carriers at dislocation states can not be uniform, as it is systematically assumed in the literature, and we propose a description of this linear charge density as a function of the dislocation energy state position and of the various features characterizing the quantum well. Using the scattering potential induced by such a spatially-dependent dislocation charge density together with the usual scattering mechanisms allows us to give an estimation of their effect on the free carriers' mobility. We particularly show that at low carrier density ($\sim 10^{12}$ cm^{-2}) the mobility is mainly determined by the combination of dislocation scattering mechanisms and intrinsic scattering mechanisms. Finally we suggest that our model could be employed for determining the position of the dislocation energy level in the gap.

(Some figures in this article are in colour only in the electronic version)

1. Introduction

AlGaN/GaN heterostructures possess attractive electronic and mechanical properties, which make them interesting for being implemented in the production of devices capable of high performance and able to work in hostile environments. One of their most unusual features is the presence, at the AlGaN/GaN interface, of a two-dimensional electron gas (2DEG) with carrier densities n_s as high as 10^{13} cm^{-2}, even in nominally undoped materials. Such a property suggests that AlGaN/GaN quantum wells (QW) should be characterized by extremely high channel currents (that could lead to the realization of record high-power devices) if good two-dimensional (2D) carrier mobility is achieved too. A lot of experimental and theoretical work is devoted to the understanding of the electronic properties of this quantum well, but also to the characterization of the interface defects and to the understanding of the way they may interact with the electrons limiting their 2D mobility. In some of the authors' previous studies about transport in AlGaN/GaN quantum wells [1, 2],

[1] Present address: Institut d'Electronique Fondamentale, Université Paris Sud, Bât. 220—Centre scientifique d'Orsay, 91405 Orsay, France.

the effect of the interface defects (like misfit dislocations, surface cracks, alloy reordering etc), originated by the relaxation of the strain energy accumulated in the AlGaN top layer, was referred to as 'interface electrical roughness', because of the non-uniform charge distribution induced by such defects at the interface. The results showed that this scattering mechanism contributes to the room temperature mobility drop at high electron concentration.

Other extrinsic scattering mechanisms that may influence the QW electron mobility are those associated with the effect of threading defects piercing the well and originating on the GaN side of the heterostructure. Such defects have been observed by TEM [3, 4], in wurtzite GaN, and they include dislocations, isolated or organized in 'columnar structures', 'nanopipes' and inversion domains with a density sometimes as high as 10^{10} cm^{-2}. They are generated at the early stages of the heteroepitaxial growth process and they are due to the high lattice mismatch between the wurtzite GaN and all available substrates (sapphire, SiC, Si). The majority of defects are dislocations occurring with a density as high as 10^{8}–10^{10} cm^{-2} [5–9] even at the top GaN surface. They appear during the nucleation mechanism when two neighbouring GaN islands, characterized by slight misorientations between them, coalesce [10–12]. In wurtzite GaN, c-screw, a-edge and $c+a$-mixed dislocations, with Burgers vectors respectively $\mathbf{b}_c = \langle 0001\rangle$, $\mathbf{b}_a = 1/3\langle 1\bar{2}10\rangle$, $\mathbf{b}_{c+a} = 1/3\langle \bar{1}\bar{1}23\rangle$, are observed [8]. However, the large majority of dislocations are of the edge and mixed type, as shown by various experimental observations (see [13] and others cited above), and each type may belong to three different 'families' corresponding to the three possible orientations of $\mathbf{b}_a$ and $\mathbf{b}_{c+a}$ in the wurtzite structure. Moreover, edge type dislocations belonging to the same family can appear isolated as well as arranged together in low-angle sub-grain boundaries, thus forming a columnar structure [14, 15].

In this paper we devote our study to the effect of threading dislocations on transport phenomena at the AlGaN/GaN heterojunction. In this order, we need to consider the mechanisms of interaction between the various types of dislocations and electrons and to interpret them in terms of scattering potentials. Thus, on one hand we derive an expression for the anisotropic deformation potential, on the other hand we propose a formulation that describes how the motion of the electrons in a well is influenced by the 'core effect' and we discuss the physical origin of this potential (section 2). In section 3, we report the results of mobility calculations in AlGaN/GaN quantum wells for various positions of their expected energy states within the GaN band gap and for various dislocation densities and we discuss them.

2. Dislocations scattering mechanisms

2.1. Introduction

Dislocations can affect transport phenomena by means of two different physical processes: (i) the local deformation that they induce in the crystal lattice and (ii) the accumulation of charge along the dislocation line.

The dislocation strain field creates a displacement of crystal atoms from their equilibrium positions, which can influence directly the electron motion in two manners: on the one hand the conduction band minimum shifts along the energy axis, inducing the formation of a deformation potential [16]; on the other hand, in non-centrosymmetric materials, the distortion field can cause the polarization of the unit cell and thus the formation of a piezoelectric potential. Even if GaN is a non-centrosymmetric material, the threading dislocations strain field $\varepsilon(x, y)$ is only dependent on the (x, y) basal coordinates, and consequently cannot introduce any piezoelectric potential in the crystal, owing to the particular shape of the piezoelectric tensor in wurtzite structures [17]. Thus only deformation potential has to be taken into account for this study.

Dislocations may also influence the electron motion if they introduce acceptor electronic states in the GaN band gap. In that case, these states act as electron traps, so as the dislocation becomes a charged line and scatters the conduction electrons by a Coulomb potential.

Both experimentally and theoretically it is quite a complex problem to determine if dislocations induce the formation of levels in the GaN band gap and which are the physical mechanisms that could lead to that. Actually there is experimental evidence of the existence of levels in the GaN band gap, but it is still controversial if they are due to dislocations or to other defects. For instance many authors reported on the observation of a highly energetic yellow luminescence (YL) (∼2.2 eV), which indicate the existence of deep gap states. Anyway the studies reported in [18, 19] showed that dislocations are not responsible for the YL, and the ones in [20, 21] proposed that the YL cannot be due to simple dislocations, but it could derive from point defects which nucleate at the dislocation core or from dislocations low-angle grain boundaries. Moreover some studies [22] showed also the existence of shallow states in the gap, but their origin is also controversial. Meanwhile other measurements by electron holography [23, 24] or by scanning capacitance microscopy [25] proved that dislocations can be negatively charged lines. This was also confirmed by the theoretical study of Wright and Grossner [26] which supports the idea that dislocations are responsible for certain extrinsic levels in the energy gap. An indirect evidence of the existence of dislocation states was also proposed in [15] as an explanation of the carrier mobility collapse observed in n type bulk GaN and it was concluded that the dislocation energy levels should correspond to shallow acceptor states localized at about 200 meV below the conduction band. This value was also confirmed by the electron energy loss study of dislocations in GaN [27] which were interpreted by the presence of a peak at about 3.2 eV above the valence band (i.e. 200 meV below the conduction band) in dislocated regions.

At first sight, the physical origin of dislocation states can be ascribed to the dislocation core atoms that do not possess the same number of first neighbours as the bulk ones and are thus decorated by dangling bonds. However, such a configuration, which would lead to the creation of amphoteric states in the gap, is anyway not energetically favoured. As a matter of fact,

the core atomic bonds would more likely tend to reconstruct among themselves, as was confirmed by various *ab initio* calculations that were performed in order to determine the dislocation core structure. For instance, Blumenau *et al* [28] found that the lowest energy structures are full-core edge and open-core screw dislocations, where the core Ga (N) atoms orbitals develop hybridizations, which clear the gap from deep levels and leave only near band edge states. Since shallow states can only issue from long-range binding potentials, their origin cannot be reasonably attributed to core atom orbitals, which would lead, instead, to a strongly localized effect. Therefore, the lattice distortion, introduced by the dislocation strain field and self-consistently taken into account in the *ab initio* calculations, may be supposed to be at the origin of the shallow states in the gap. This hypothesis was proposed and confirmed in the works presented in [29, 30], that solved both numerically and analytically the Schrödinger equation of the envelope function in the presence of the dislocation strain field binding potential and found that these circumstances lead to the formation of shallow one-dimensional bands for both electrons and holes in the energy gap. According to [29, 30], in GaN, the electronic bound states due to the dislocation deformation potential should lie at ∼100 meV below the conduction band. Also, this last result was confirmed through *ab initio* calculations performed on big clusters (∼60 000 atoms) [31], which showed that the core orbitals are fully reconstructed leading to core structures in agreement with HR-TEM pictures and eliminating the possible existence of any deep states. Only empty shallow states below the conduction band were found and attributed to the deformation field of the dislocation.

From the above discussion, we consider that the most realistic picture for the dislocation energy states corresponds to empty shallow states localized at about 100–200 meV below the conduction band. These states being closely and periodically located along the dislocation line they act as a 1D band. As a consequence, some electrons can be trapped by this dislocation 1D band, transforming it into a charged line that acts as a 1D Coulomb scattering centre. Such a scattering mechanism associated with trapped electrons is commonly referred to as the 'core effect'. In the present study, we calculate the effect of both types of scattering mechanisms (deformation potential and Coulomb potential) on the free carrier mobility in AlGaN/GaN quantum wells.

It is worth noticing that the strain field of pure screw dislocations does not introduce any dilatation part, so that they cannot act on the carrier mobility through the deformation potential. For the same reason, they cannot even couple shallow levels and, therefore, the core effect associated with c-screw dislocations can be ruled out. On top of that, screw dislocations are present in GaN in a far lower concentration than edge dislocations, thus their effect, if any, is anyway negligible. Therefore, in the present approach, we consider that only a-edge dislocations, as well as the edge component of $c+a$-mixed dislocations, may act as electron scattering centres.

2.2. Deformation potential

The deformation potential associated with the dilatation part of the strain field induced by a dislocation in the crystal was derived by Dexter and Seitz [16] in analogy with the one introduced by Bardeen and Shockley [32] for acoustic phonon scattering. In the case of direct gap semiconductors and for dislocations whose lines are parallel to the c axis of the wurtzite structure, the unscreened deformation potential energy created by a single dislocation is expressed by

$$W_{1\text{disloDP}}(\vec{\rho}) = E_1 \,\mathrm{Tr}[\varepsilon(x, y)] \tag{2.1}$$

where E_1 is the basal diagonal coefficient of the deformation potential energy tensor and $\vec{\rho} = (x, y)$ a 2D space vector. The trace of the strain tensor $\mathrm{Tr}[\varepsilon(x, y)]$, for an edge dislocation, in the isotropic elastic medium approximation, is given by [33]

$$\mathrm{Tr}[\varepsilon(x, y)] = \frac{(1-2\upsilon)}{2\pi(1-\upsilon)} \frac{\vec{b} \times \vec{\rho}}{\rho^2} \tag{2.2}$$

with **b** the dislocation Burgers vector and υ the Poisson coefficient of the isotropic medium. The 2D Fourier transform of this potential energy is

$$\tilde{W}_{1\text{disloDP}}(q) = \mathrm{i} \frac{E_1(1-2\upsilon)b}{(1-\upsilon)} \frac{\sin\alpha}{q} \tag{2.3}$$

where α is the angle between the Burgers vector and the 2D **q** wavevector. The matrix elements corresponding to the deformation potential energy created by a random distribution of dislocations and calculated between the various $|n, k\rangle$ states of the quantum well (n being the subband index and k the 2D wavevector) are

$$\langle n, \vec{k}|W_{\text{DP}}(\vec{\rho})|n', \vec{k}'\rangle = \sum_j \langle n, \vec{k}|W_{1\text{disloDP}}(\vec{\rho} - \vec{\rho}_j)|n', \vec{k}'\rangle$$

$$= S(q)\tilde{W}_{1\text{disloDP}}(q) \frac{\delta_{\vec{k}', \vec{k}+\vec{q}}}{S} \delta_{n,n'} \tag{2.4}$$

where $S(q) = \sum_j \exp(\mathrm{i}\vec{q} \cdot \vec{\rho}_j)$ is a 'sub-structure' factor, whose square modulus is equal to the number of dislocations N_{dislo}, if a random distribution of dislocations is assumed. From expression (2.4) we clearly see that inter-subband transitions are not allowed when electrons interact with the deformation potential created by dislocations having their line parallel to the c axis of the wurtzite structure (i.e. orthogonal to the AlGaN/GaN interface plane). In real crystals, threading dislocations may have their lines not exactly parallel to the c axis, thus giving rise to inter-subband transitions. However this is a small contribution that we neglect here.

The angle α appearing in (2.3) depends on the three possible orientations of the Burgers vector of the edge dislocation. In order to determine the scattering potential of an ensemble of dislocations uniformly distributed among the three families of **a**-type Burgers vector (so-called 'as-grown' dislocations, because anyone orientation of the **a**-type Burgers vector is favoured during the growth process), one has to calculate the screened square of the matrix element (2.4) for each orientation of the Burgers vector assuming that $|S(q)|^2 = N_{\text{dislo}}/3$ (uniform distribution of dislocations). Summing up

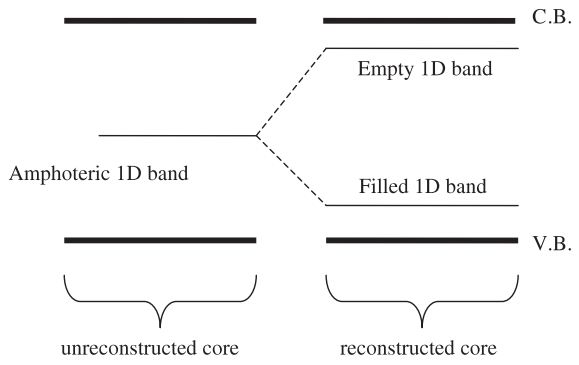

Figure 1. Schema of possible dislocation states configurations in bulk GaN: 1D amphoteric band or 1D shallow empty and filled bands.

these three screened squared matrix elements, the angular dependence disappears and it is statistically replaced by a factor 1/2. Therefore we can straightforwardly write just one matrix element associated with the deformation potential created by a random distribution of as-grown edge dislocations as follows

$$\langle n, \vec{k}|W_{\mathrm{DP}}(\vec{\rho})|n', \vec{k}'\rangle = \mathrm{i}\sqrt{\frac{N_{\mathrm{D}}}{2}}\frac{E_1(1-2v)}{S(1-v)}\frac{b}{q}\delta_{\vec{k}',\vec{k}+\vec{q}}\delta_{n,n'}. \tag{2.5}$$

Notice that, due to the symmetric orientation of the three edge Burgers vector, this result could be found also by directly calculating the average value $\langle \sin\alpha^2\rangle = 1/2$.

2.3. 'Core effect' scattering

The main conclusion of section 2.1 is that the dislocation core is reconstructed, which leads to the formation of a shallow acceptor energy band, lying at ∼100–200 meV below the conduction band. However, the scattering potential models widely used in literature are based on the different assumption that the dislocation core is unreconstructed and that the dangling orbitals induce the formation of a 1D deep amphoteric level in GaN. In the present work we want to develop a model supposing that some core reconstruction takes place and that the amphoteric band splits into a shallow empty band, localized below the conduction band, and a filled band, localized above the valence band, as shown in figure 1. The position in the gap of the shallow level will be taken in our model as an open parameter. As soon as a quantum well is formed, the dislocations 1D band bends near the interface, leading to the configurations shown in figures 2(a) and (b), for the case of amphoteric and shallow bands, respectively. As a consequence, a part of the dislocation energy states may go below the Fermi level and electrons are more likely to be trapped on such states. This results in the formation of a linear charge distribution having a space-dependent density $\lambda(z)$, which, far from the interface, tends towards the linear density in bulk materials λ_{bulk}. This value depends on the dislocation states occupation rate, which is statistically self-regulated by the electrostatic interaction between carriers trapped on

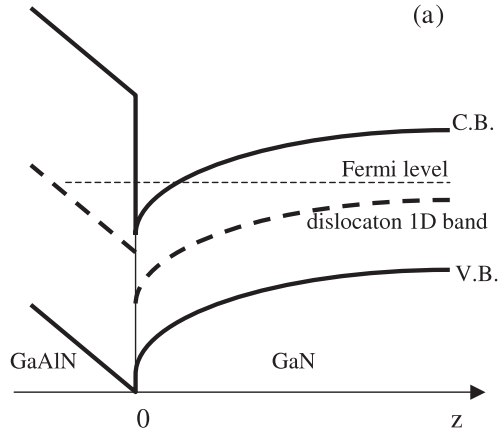

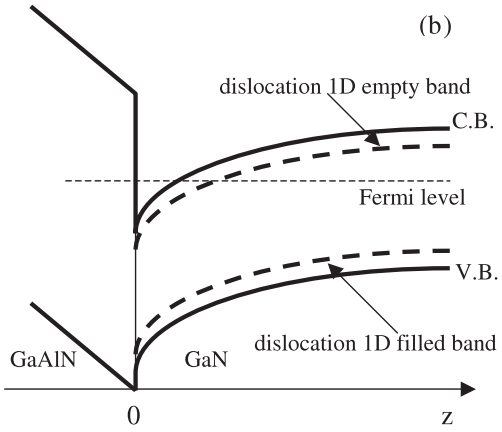

Figure 2. (a) Schematic representation of the dislocation amphoteric band bending at the AlGaN/GaN interface; in GaN, all dislocation states are located well below the Fermi level so that the dislocation line may be approximately considered as a uniformly charged line. (b) Schematic representation of the dislocation states issued from core reconstruction; only a small part of dislocation states are located below the Fermi level and electrons are more likely to be trapped on such states, thus giving to the dislocation occupied states a 'quantum segment' character.

neighbouring sites [34, 35]. For instance, in homogeneous 3D systems, it was shown [36] that the linear density is given by

$$\lambda_{\mathrm{bulk}} = \frac{2e}{d}\left(\frac{1}{1+\mathrm{e}^{(E_{\mathrm{D}}^*-\varepsilon_{\mathrm{F}})/KT}} - \xi\right) \tag{2.6}$$

where ξ is the electronic occupancy of the neutral dislocation (typically 1/2 for an amphoteric band and zero for an empty band), d is the distance between two neighbouring dislocation sites and E_{D}^* is the 'effective' dislocation energy level given by

$$E_{\mathrm{D}}^* = E_{\mathrm{D}} + W_{\mathrm{int}} = E_{\mathrm{D}} + \frac{e\lambda_{\mathrm{bulk}}}{2\pi\varepsilon_0\varepsilon_L}\left(\ln\left(\frac{d_{\mathrm{sc}}}{d}\right) - \frac{1}{2}\right) \tag{2.7}$$

with E_{D} the neutral dislocation energy state, W_{int} an energy shift issued from the interaction among trapped electrons and d_{sc} the 3D screening length.

In the academic (and probably non-realistic) case of an unreconstructed amphoteric dislocation, one may imagine a

dislocation deep energy state E_D of the order of $E_{gap}/2$ below the conduction band. Since GaN is a wide band gap semiconductor, this would lead to an extremely large (and therefore practically z independent) linear charge density λ, of the order of $\sim$1 electron each d distance, even if the interaction between trapped electrons is taken into account. This assumption, $\lambda(z) =$ constant, leads to a simple situation where the matrix element of the unscreened Coulomb scattering potential energy, created by a random distribution of dislocations, is given by

$$\langle n, \vec{k}|W_{core}(\vec{r})|n', \vec{k}'\rangle = S(q)\frac{e\lambda}{S\varepsilon_0\varepsilon_L q^2}\delta_{\vec{k}',\vec{k}+\vec{q}}\delta_{n,n'} \qquad (2.8)$$

where $S(q)$ is as defined in section 2.2. Up to now, this potential matrix element, as well as some equivalent formulation based on a z independent linear charge density of the dislocation, has been widely used in various papers considering the dislocation scattering in nitrides (see for instance [37, 38]). Note that this potential does not allow taking into account inter-subband transitions.

In a more realistic situation where some reconstruction takes place (as shown in figure 2(b)), the dislocation may certainly not be considered as an homogeneously charged line and its space-dependent linear charge density $\lambda(z)$ has to be determined prior to any transport calculation. In this order we may consider the Hamiltonian of the electronic system in the presence of a neutral dislocation

$$H = H_0 + eV_{QW}(z) + eV_{dislo}(x, y) \qquad (2.9)$$

where $V_{dislo}(x, y)$ is the dislocation binding potential and $V_{QW}(z)$ is the quantum well potential.

The electrons feel the confining effect of these two potentials and, the (x, y) and z coordinates being independent, their wavefunctions and energy states are given by

$$\Psi(x, y, z) = \varphi_{dislo}(x, y)Z_n(z) \qquad (2.10)$$

$$E_{D,n} = \varepsilon_n + E_D \qquad (2.11)$$

where $Z_n(z)$ are the quantum well wavefunctions and ε_n their corresponding energy eigenstates and E_D is the dislocation energy state. This means that a dislocation piercing the quantum well acts on the electrons as a quantum box (or, more exactly, as a 'quantum segment') whose total charge density distribution is given by

$$\rho(r) = 2e|\varphi_{dislo(x,y)}|^2 \sum_n |Z_n(z)|^2 f(\varepsilon_n + E_D + W_{int}[\rho(r)]). \qquad (2.12)$$

The occupation function f entering the above expression depends on the contribution $W_{int}[\rho(r)]$ of the electrostatic interaction energy between trapped carriers, in a manner similar to expression (2.7). However, the evaluation of this interaction energy would require the determination of the (x, y)-dependent wavefunction as well as a self-consistent solution of equation (2.12). Therefore, we prefer to develop an approximated analytical model able to take into account the main features of expression (2.12). We assume that trapped electrons are perfectly confined along the dislocation line and

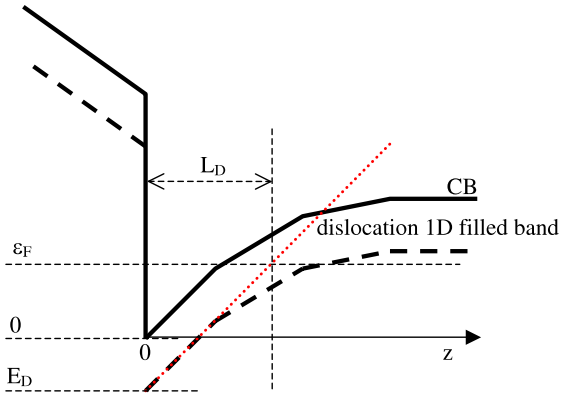

Figure 3. Schematic diagram illustrating the calculation of the parameter L_D.

that the 1D charge density distribution along the dislocation line $\lambda(z)$ has to go continuously from a value $\lambda_0 = \lambda(z = 0)$, at the interface, to $\lambda_{bulk} = \lambda(z = \infty)$, in the bulk GaN, using an arbitrary law, as for instance

$$\lambda(z) = \begin{cases} \lambda_{bulk} + (\lambda_0 - \lambda_{bulk})e^{-z/L_D} & \text{for } z \geqslant 0 \\ 0 & \text{for } z < 0 \end{cases} \qquad (2.13)$$

where λ_{bulk} is given by expression (2.6). The choice $\lambda(z) = 0$ for $z < 0$ is justified by the fact that the dislocation line continuing in the AlGaN top layer also induces shallow states, that probably lie above the Fermi level, and therefore are empty, owing to the particularly wide band gap of AlGaN. The linear density λ_0 obtained at $z = 0^+$ may be evaluated by assuming that, at this point, the dislocation energy states are far below the Fermi level so that they should be occupied at their maximum (i.e. two electrons per dislocation energy state) leading to a maximum value for λ_0. However, the electrostatic interaction energy between trapped carriers tends to self-regulate the occupation statistics: here we take into account such an effect by simply weighting the maximum charge density by a filling factor $0.5 < \gamma < 1$, so that $\lambda_0 = \gamma\lambda_{max}$ ($\gamma = 0.5$ describes a half filled state and $\gamma = 1$ describes a fully occupied state). Considering the core of a dislocation as a 1D crystal of length L and of lattice period d, the number of allowed states on the corresponding energy band is L/d which allows us to estimate the maximum value of the linear charge density to $\lambda_{max} = 2e/d$ (two electrons per state). We must notice that due to the necessary continuity with the surrounding crystal, the period along the dislocation line cannot change even if some core reconstruction takes place, so that the period d is equal to the c_0 length of the unit cell of wurtzite structure.

In expression (2.13), L_D is a typical length separating the dislocation portion that can be considered to feel the QW potential from the one lying in the 3D continuum. As shown in figure 3, the L_D parameter may be estimated as the distance between the origin of the Oz axis and the point z corresponding to the intersection of the Fermi level ε_F with the following potential energy

$$W(z) \equiv E_D + eV_{QW}(z) = E_D + \frac{e\sigma}{2\varepsilon_0\varepsilon_L}z \qquad (2.14)$$

which represents the potential energy of a triangular quantum well $eV_{QW}(z)$ (σ is the 2D density of the interface charge and it is assumed to be equal to the 2DEG charge density), shifted by the E_D dislocation binding energy. Thus

$$L_D \equiv \frac{2\varepsilon_0\varepsilon_L}{e\sigma}(\varepsilon_F - E_D). \tag{2.15}$$

Obviously, the choice of the $\lambda(z)$ function (2.13) as well as that of the L_D value are somehow arbitrary, but they have the merit to take into account the dislocation main features as well as the quantum well ones. The use of (2.13) to express $\lambda(z)$ was also motivated by the fact that its Fourier transform is simple and leads to the following unscreened matrix elements for the Coulomb potential energy created by a random distribution of dislocations

$$\begin{aligned}\langle n, \vec{k}|W_{core}(\vec{r})|n', \vec{k}'\rangle &= S(q)\frac{e\lambda_{bulk}}{2S\varepsilon_0\varepsilon_L q^2}\delta_{\vec{k}',\vec{k}+\vec{q}}\delta_{nn'} \\ &+ S(q)\frac{e(\lambda_0-\lambda_{bulk})L_D}{S\varepsilon_0\varepsilon_L 2\pi}\delta_{\vec{k}',\vec{k}+\vec{q}} \\ &\times \int_{-\infty}^{\infty}\frac{(1+iq_zL_D)G_{nn'}(q_z)}{(1+q_z^2L_D^2)(q^2+q_z^2)}\,dq_z \end{aligned}\tag{2.16}$$

where we have introduced the form factor

$$G_{nn'}(q_z) = \int_{-\infty}^{\infty} Z_n^*(z)Z_{n'}(z)\,e^{-iq_zz}\,dz \tag{2.17}$$

and where $S(q)$ is as defined in section 2.2. We note that the first term of the right side of expression (2.16) corresponds to the usual matrix element (2.8) but contains a supplementary factor $1/2$ that issues from the fact that we suppose the dislocation line to be uncharged in the AlGaN top layer. Moreover its contribution takes into account the linear charge density λ_{bulk} calculated in the bulk GaN through the use of expressions (2.6) and (2.7) and will not be systematically equal to a maximum value e/d as it is assumed in the usual models. The presence of the form factor $G_{nn'}(q_z)$ in the second term results from the z-dependence of the dislocation charge and indicates that inter-subband contributions are expected. The second term also possesses an imaginary contribution which will lead to some interference with the deformation potential contribution (2.4), which is totally imaginary.

Both expressions (2.5) and (2.16) correspond to the unscreened matrix element of the scattering potential. The corresponding screened values, employed for mobility determination, are obtained by making use of the procedure described in [39].

3. Results and discussion

In order to determine to what extent threading dislocations contribute to the reduction of the maximum 'intrinsic' mobility expected in AlGaN/GaN QWs (see [40, 41]), we calculated the room temperature 2D electron mobility, as a function of the carrier density, considering the combination of intrinsic scattering mechanisms (acoustic phonons and polar optical phonon/plasmon hybrid particles) with the dislocation scattering mechanisms (both deformation potential and core effect included). The electron envelope functions $Z_n(z)$ used in the calculations are the wavefunctions of an infinite triangular quantum well and are determined numerically following the procedure described in [1, 2]. Inter-subband transitions are taken into account as previously done in [39, 40]. Quantities needed for a numerical evaluation of the dislocation potentials are standard tabulated GaN parameters (like magnitude of the Burgers vector, the conduction band effective mass, the Poisson's ratio and the deformation potential constant) and the dislocation density, which from experimental observations is known to range between 10^8 and 10^{10} cm^{-2}. The dislocation energy level E_D has been considered as an open parameter ranging between 100 and 300 meV as well as the filling factor $0.5 < \gamma < 1$ entering the dislocation linear charge density at $z = 0$, $\lambda_0 = 2e/c_0\gamma$. In particular, we combined the average deformation potential (2.5) with the core effect potential (2.16) for various positions of the dislocation level, and for a dislocation density of 8×10^8 cm^{-2}. Results are shown in figure 4 for the limiting values $\gamma = 1$ and 0.5. Experimental values of mobility taken from [42] and measured on an AlGaN/GaN gated Hall bar (sample T799) having a dislocation density of 8×10^8 cm^{-2} and a 2DEG density of 7.6×10^8 cm^{-2} are shown in figure 4 too. We can notice that the deformation potential alone does not introduce any important variation of the intrinsic mobility. On the contrary, scattering due to core effect is extremely effective and strongly lowers the free carrier mobility at low carrier density ($n_s < 6$–8×10^{12} cm^{-2}). We can make

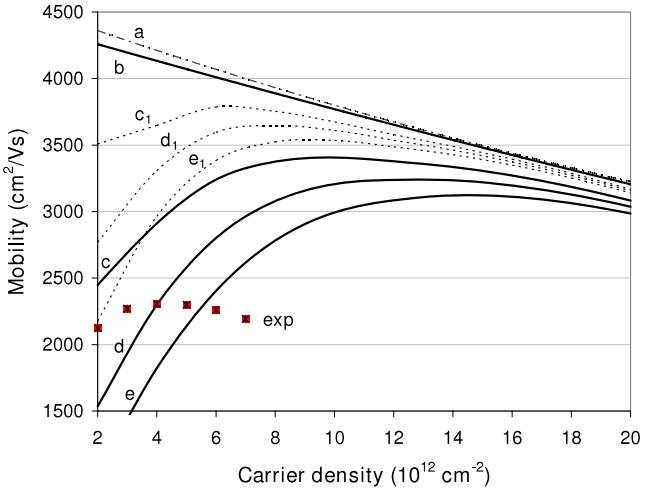

Figure 4. Room temperature free carrier mobility versus carrier density limited by the dislocation scattering (deformation and core effect) combined with intrinsic diffusion potentials (acoustic phonons and polar optical phonon/plasmon hybrid particles). The various curves are calculated for a dislocation density equal to 8×10^8 cm^{-2}, for various positions of the dislocation energy level below the conduction band and for the two limiting values of the filling factor $\gamma = 1$ and 0.5. Curve (a) is calculated taking into account intrinsic scattering mechanisms only; curve (b) contains the effect of the deformation potential created by dislocations; curves (c), (d), (e) ($\gamma = 1$) and (c_1), (d_1), (e_1) ($\gamma = 0.5$) are determined introducing the dislocation core effect, for dislocation energy levels located respectively at 100, 200, 300 meV below the conduction band. Square markers refer to experimental values (sample T799 of [42]).

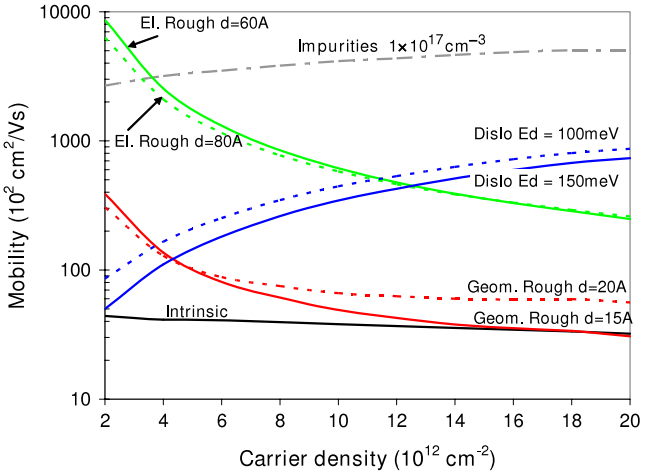

Figure 5. Room temperature free carrier mobility versus carrier density, limited by individual scattering mechanisms. Geometrical and electrical covering ratios are chosen as 25%; the average charge variation is chosen as 25% of intrinsic 2DEG charge; the island thickness is taken as 1 monolayer. The dislocation density is 8×10^8 cm^{-2} and the filling factor is $\gamma = 1$.

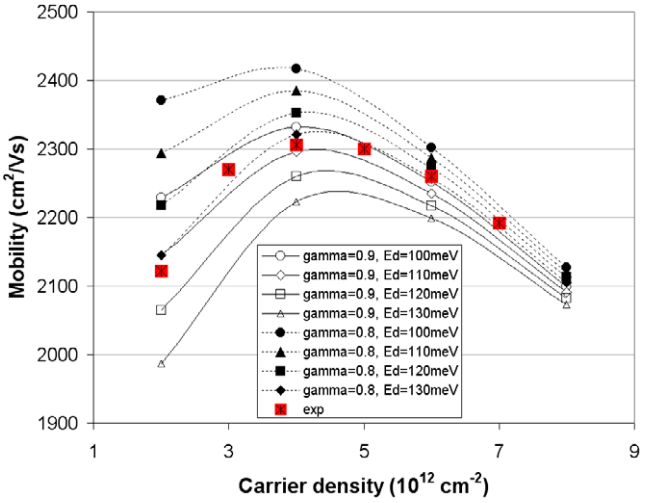

Figure 6. Room temperature free carrier mobility versus carrier density. The theoretical calculations take into account the combined effect of intrinsic scattering mechanisms (acoustic phonons and optical phonon/plasmon hybrid particles), residual impurities, interface geometrical roughness and interface electrical roughness, dislocations (deformation potential and core effect). Characteristic parameters of interface roughness are the same in all curves, while the γ (gamma) filling factor and the dislocation energy level *Ed* are varying. The experimental values are measures carried on a gated Hall bar (sample T799 of [42]).

the following remarks:

(i) In the whole carrier density range, the mobility strongly decreases as soon as the dislocation level goes deeper below the conduction band. This is a direct consequence of our model, since the deeper the dislocation energy state, the longer the portion of the dislocation band lying below the Fermi level. Such an effect could not be obtained in usual models, which considered a linear dislocation charge density arbitrarily chosen equal to its maximum value $\lambda = e/d$, independently of the dislocation energy state position.

(ii) The dislocation scattering appears to be strongly dependent on the carrier density, leading to very low mobility at low carrier density. Such a trend was also noticed in the previous models since it is partially a consequence of the free carrier screening whose strength increases with increasing carrier density. However, in the present approach, this dependence is much more pronounced than in usual models since, beyond the screening effect, as the carrier density rises, the dislocation band portion lying below the Fermi level becomes shorter, thus reducing the strength of the scattering potential.

(iii) Comparing theoretical and experimental results, we can observe that the upper limit for the dislocation energy level (i.e. the deepest position below the conduction band) range about 300 meV if we take γ equal to its smallest value 0.5. As a matter of fact, a stronger dislocation potential would lead to a theoretical mobility lower than the experimental one, even without taking into account other extrinsic scattering mechanisms. Moreover, notice that in our model γ should be only a small correction to take into account the self-regulation of the dislocation occupation statistics and thus higher values like $\gamma = 0.8$–0.9 would be more appropriate. In that case the dislocation energy level should range between 100 and 200 meV to get a theoretical mobility higher than the measured one. We can conclude that the comparison between the results of our calculations and the results of measurement allows us to confirm that dislocations introduce shallow levels in the GaN energy gap.

Employing this model of dislocation scattering potential in our mobility simulations allows us to reproduce well the measured mobility variation as a function of carrier density. We took into account the combined effect of intrinsic scattering mechanisms, dislocations, uniform distribution of residual impurities, geometrical interface roughness and electrical interface roughness. Usually, residual impurity concentration is quite low ($N_{\text{imp}} = 10^{17}$ cm^{-3}) and its effect on mobility is far lower than the one of other scattering mechanisms as we can see from figure 5. The models used for geometrical and electric interface roughness are those of [2]: they depend on various parameters like covering ratio, correlation length, island thickness characteristic of geometrical roughness and covering ratio, correlation length and average local charge variation characteristic of electrical roughness. The geometrical roughness efficiency is quite large and comparable to that of dislocations, except that its strength increases with increasing carrier density, contrarily to the case of dislocations (see figure 5). Thus, the mixture of both scattering mechanisms allows one to reveal some well marked maximum in the mobility versus density curve. Then, even if the exact position of the mobility maximum depends on the parameters used for the description of both interface roughness and dislocations, the slope of the mobility versus carrier density curve obtained at low carrier density is mainly determined by the choice of the dislocation density and dislocation model parameters. In figure 6 are shown some results of our calculations as well

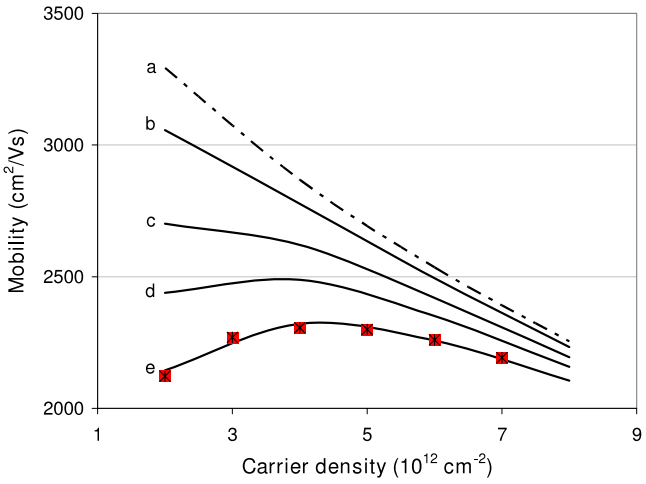

Figure 7. Room temperature free carrier mobility versus carrier density. Curve (a) is calculated taking into account intrinsic scattering mechanisms only. Curve (e) reproduces the experimental results of [42] for sample T799 that are as shown by square markers. Curves (b), (c), (d), are calculated using the same parameters employed for the curve (b), but the dislocation density is respectively 1×10^8, 3×10^8, and 5×10^8 cm^{-2}.

as the results of measurements carried on an AlGaN/GaN gated Hall bar taken from [42] (sample T799). We adjusted the ensemble of interface roughness parameters in order to reproduce the order of magnitude of experimental mobility at high carrier density (i.e. $n_s = 6$–8×10^{12} cm^{-2}), for a given dislocation density (8×10^8 cm^{-2}), for a dislocation energy level $Ed = 100$–200 meV, and for $\gamma = 0.8$–0.9 in order to give an account of a small interaction energy between trapped electrons. The parameters used for the interface roughness are as follows: geometrical covering ratio is set up to 25%, geometrical correlation length to 14 Å, island thickness to 1 monolayer, electrical covering ratio to 25%, electrical correlation length to 60 Å, and average charge variation to 25% of the intrinsic 2DEG density. Note that an ensemble of slightly different values may lead to the same result, however a far lower or far higher value of correlation length would drastically reduce the effect of interface roughness and no longer allow the reproduction of the experimental mobility at high carrier density. At the same time, by varying the dislocation parameters we adjusted our theoretical results to the experimental ones and a quite good agreement over the whole carrier density range may be found, for example with the choice $Ed = 130$ meV and $\gamma = 0.8$. Obviously these values are not univocally determined, but they may vary slightly if interface roughness parameters are correspondingly adjusted. We have to point out that the variation of the QW shape due to the application of a gate bias is reproduced in our calculation by varying the 2D charge density that creates the infinite triangular QW, which is assumed to be equal to the 2DEG density. On the contrary, the interface charge fluctuation responsible of electrical interface roughness is obviously kept constant in all calculations.

We then used the ensemble of parameters that allowed us to reproduce experimental results to give an estimation of the maximum dislocation density that should be achieved in heterostructures in order to limit the effect of dislocation on electron mobility degradation. As we can see in figure 7 the achievement of a maximum dislocation density of 10^8 cm^{-2} would allow their detrimental effect on mobility to be restrained mainly to the low carrier density region ($n_s < 4 \times 10^{12}$ cm^{-2}).

It is worth noticing that our core effect dislocation model may provide a method for exactly determining the dislocation energy level position provided that the interface roughness parameters may be estimated from experimental observations (mainly the covering ratio) or fixed by other complementary studies (mainly the correlation length) like low temperature quantum lifetime to relaxation time ratio measurements and theoretical evaluation.

4. Conclusion

We have developed an original model for the scattering potential created by the so-called dislocation core effect for the specific case of threading dislocations in QWs. Our model is based on the consideration that threading dislocations in GaN may only create shallow energy states. Therefore in AlGaN/GaN QWs, due to the bending of the dislocation band, electrons are not uniformly trapped on the dislocation states. Thus we propose a model taking into account the non-uniform linear charge distribution trapped along the dislocation line as well as the bending of the dislocation band. We show that our model allows us to reproduce experimental mobility as a function of carrier density when we calculate the mobility limited by the combined effect of intrinsic scattering mechanisms, dislocations, residual impurities and interface roughness. It is shown that the dislocation deformation potential has a very low effect. We give an estimation of the maximum dislocation density that should be achieved in order to almost remove the effect of dislocation on mobility at high carrier density ($n_s > 5 \times 10^{12}$ cm^{-2}). The dislocation energy level being an open parameter of the model, we suggest that our model may provide a way to get its exact estimation once the interface roughness parameters are known. The present results confirm that dislocations introduce shallow states in the energy gap of GaN.

References

[1] Farvacque J-L, Bougrioua Z, Carosella F and Moerman I 2002 *J. Phys.: Condens. Matter* **14** 13319
[2] Farvacque J-L and Bougrioua Z 2003 *Phys. Rev.* B **68** 035335
[3] Cherns D, Young W T and Ponce F A 1997 *Mater. Sci. Eng.* B **50** 76
[4] Cherns D 2000 *J. Phys.: Condens. Matter* **12** 10205
[5] Lester S D, Ponce F A, Crawford M G and Steigerwald D A 1995 *Appl. Phys. Lett.* **66** 1249
[6] Qian W, Skowronski M, Degaref M, Doverspike K, Rowland L B and Gaskill D K 1995 *Appl. Phys. Lett.* **66** 1252
[7] Manfra M J, Weimann N G, Hsu J W P, Pfeiffer L N, West K W and Chu S N G 2002 *Appl. Phys. Lett.* **81** 1456
[8] Germain M, Leys M, Boeykens S, Degroote S, Wang W, Schreurs D, Ruythooren W, Choi K-H, Van Daele B, Van Tendeloo G and Borghs G 2004 *Mater. Res. Soc. Symp. Proc.* **798** Y10.22.1

[9] Cordier Y, Hugues M, Semond F, Natali F, Lorenzini P, Bougrioua Z, Massies J, Frayssinet E, Beaumont B, Gibart B and Faurie J-P 2005 *J. Cryst. Growth* **278** 383
[10] Degave F, Ruterana P, Nouet G, Je J H and Kim C C 2002 *J. Phys.: Condens. Matter* **14** 13019
[11] Valcheva E, Paskova T and Monemar B 2002 *J. Phys.: Condens. Matter* **14** 13269
[12] Kwon Y B, Je J H, Routerana P and Nouet G 2005 *J. Vac. Sci. Technol.* A **23** 1588
[13] Hino T, Tomiya S, Miyajima T, Yanashima K, Hashimoto S and Ikeda M 2000 *Appl. Phys. Lett.* **76** 3421
[14] Ponce F A and Bour D P 1997 *Nature* **386** 351
[15] Farvacque J-L, Bougrioua Z and Moerman I 2001 *Phys. Rev.* B **63** 115202
[16] Dexter D L and Seitz F 1952 *Phys. Rev.* **86** 964
[17] Shi C, Asbeck P M and Yu E T 1999 *Appl. Phys. Lett.* **74** 573
[18] Hsu J W P, Schreyand F F and Ng H M 2003 *Appl. Phys. Lett.* **83** 4172
[19] Dassonneville S, Amokrane A, Sieber B, Farvacque J-L, Beaumont B and Gibart P 2001 *J. Appl. Phys.* **89** 3736
[20] Lei H, Leipner H S, Schreiber J, Weyher J L, Wosinski T and Grzegory I 2002 *J. Appl. Phys.* **92** 6666
[21] Ponce F A, Bour D P, Götz W and Wright P J 1996 *Appl. Phys. Lett.* **68** 57
[22] Soltanovich O A, Yakimov E B, Shmidt N M, Usikov A S and Lundin W V 2003 *Physica* B **340–342** 479
[23] Cai J and Ponce F A 2002 *Phys. Status Solidi* b **192** 407
[24] Cherns D and Jiao C G 2001 *Phys. Rev. Lett.* **87** 205504
[25] Hansen P J, Strausser Y E, Erickson A N, Tarsa E J, Kozodoy P, Brazel E G, Ibbeston J P, Mishra U, Narayanamurti V, DenBaars S P and Speck J S 1998 *Appl. Phys. Lett.* **72** 2247
[26] Wright A F and Grossner U 1998 *Appl. Phys. Lett.* **73** 2751
[27] Bangert U, Gutiérrez-Sosa A, Harvey A J, Fall C J and Jones R 2003 *J. Appl. Phys.* **93** 2728
[28] Blumenau A T, Elsner J, Jones R, Heggies M I, Öberg S, Frauenheim T and Briddon P R 2000 *J. Phys.: Condens. Matter* **12** 10223
[29] Farvacque J-L and François P 2001 *Phys. Status Solidi* b **223** 635
[30] Farvacque J-L and Pödör B 1991 *Phys. Status Solidi* b **167** 687
[31] Lymperakis L, Neugebauer J, Albrecht M, Remmele T and Strunk H P 2004 *Phys. Rev. Lett.* **93** 196401
[32] Bardeen J and Shockley W 1950 *Phys. Rev.* **80** 72
[33] Hirth J P and Lothe J 1968 *Theory of Dislocations* (New York: McGraw-Hill)
[34] Read W T 1954 *Phil. Mag.* **45** 775
Read W T 1954 *Phil. Mag.* **45** 1119
[35] Schröter W and Labusch R 1969 *Phys. Status Solidi* **36** 359
[36] Masut R, Penchina C M and Farvacque J-L 1982 *J. Appl. Phys.* **53** 4964
[37] Jena D, Gossard A C and Mishra U K 2000 *Appl. Phys. Lett.* **76** 1707
[38] Gurusinghe M N, Davidsson S K and Anderson T G 2005 *Phys. Rev.* B **72** 045316
[39] Farvacque J-L 2003 *Phys. Rev.* B **67** 195324
[40] Farvacque J-L and Carosella F 2005 *Phys. Rev.* B **72** 125344
[41] Carosella F, Farvacque J-L and Germain M 2006 *Mater. Res. Soc. Symp. Proc.* **831** E8.6
[42] Bougrioua Z, Azize M, Lorenzini P, Laügt M and Haas H 2005 *Phys. Status Solidi* a **202** 536